Laser and Particle Beams (2003), *21*, 511–516. Printed in the USA.

DOI: 10.1017/S0263034603214051

X-ray microscopy of living multicellular organisms with the Prague Asterix Iodine Laser System

T. DESAI,[1] D. BATANI,[1] A. BERNARDINELLO,[1] G. POLETTI,[2] F. ORSINI,[2] J. ULLSCHMIED,[3] L. JUHA,[3] J. SKALA,[3] B. KRALIKOVA,[3] E. KROUSKY,[3] M. PFEIFER,[3] C. KADLEC,[3] T. MOCEK,[3] A. PRÄG,[3] O. RENNER,[3] F. COTELLI,[4] C. LORA LAMIA,[4] AND A. ZULLINI[5]

[1]Dipartimento di Fisica "G.Occhialini" and INFM, Università, di Milano Bicocca, Milano, Italy
[2]Istituto di Fisiologia Generale e Chimica Biologica, Università di Milano, Milano, Italy
[3]Prague Asterix Iodine Laser System Research Centre, Prague, Czech Republic
[4]Dipartimento di Biologia, Università di Milano, Milano, Italy
[5]Dipartimento di Biotecnologie e Bioscienze, Università di Milano Bicocca, Milano, Italy

(RECEIVED 25 January 2003; ACCEPTED 19 May 2003)

Abstract

Soft X-ray contact microscopy (SXCM) experiments have been performed using the Prague Asterix Iodine Laser System (PALS). Laser wavelength and pulse duration were $\lambda = 1.314\ \mu$m and τ (FWHM) = 450 ps, respectively. Pulsed X rays were generated using teflon, gold, and molybdenum targets with laser intensities $I \geq 10^{14}$ W/cm^2. Experiments have been performed on the nematodes *Caenorhabditis elegans*. Images were recorded on PMMA photo resists and analyzed using an atomic force microscope operating in contact mode. Our preliminary results indicate the suitability of the SXCM for multicellular specimens.

Keywords: Atomic force microscopy; Laser-produced plasmas; Multicellular *Caenorhabditis elegans*; Soft X-ray contact microscopy

1. INTRODUCTION

In 2002, the Nobel prize in Physiology or Medicine was awarded to Sydney Brenner, USA, H. Robert Horvitz, UK, and John E. Sulston, USA for their seminal discoveries concerning genetic regulation of organ development and programed cell death. They used the nematode *Caenorhabditis elegans* as an experimental model to follow cell division and differentiation from the fertilized egg to an adult. While identifying the key genes, they have shown that corresponding genes exist in higher species, including man, and the discovery has shed new light on the pathogenesis of many diseases (Nobel Foundation, 2002). The importance of *C. elegans* as a model initiated the present work.

Soft X-ray contact microscopy (SXCM), this paper is devoted to the study of *C. elegans* by a technique devised to produce images of biological specimens using short wavelength radiation and provides a resolution higher than optical microscopy. With respect to other imaging techniques, such as electron microscopy (EM), it avoids the drawbacks of sample preparation. In EM, the specimens must be fixed, dehydrated, embedded in resin, cut in thin sections, and stained with heavy metals. Potentially any of these processes may introduce artifacts (Ford *et al.*, 1992) and thus the possibility of studying living samples is precluded. SXCM allows living organisms to be imaged in a liquid environment (Ford *et al.*, 1991; Fletcher *et al.*, 1992), also allowing an easier way of handling the samples. SXCM experiments exploit the existence of a particular region of the electromagnetic spectrum, called the Water Window (WW), which lies between the absorption edges of carbon (280 eV) and of oxygen (530 eV). In the WW region, water is almost transparent to X-rays, whereas carbon, which is the main constituent of the organic structures, is highly opaque. Therefore it is possible to produce high contrast images in organic samples.

Laser plasmas seems to be an ideal X-rays source for SXCM (Stead *et al.*, 1995*a*). The hot and dense plasma produced in the interaction of a laser pulse with a solid target (Kondo & Tomie, 1994) can yield high fluxes of radiation whose spectrum can be chosen by changing the target material and the beam focusing. The short irradiation time of the order of the laser pulse is far below the time needed (of

Address correspondence and reprint requests to: Tara Desai, Dipartimento di Fisica "G. Occhialini" and INFM, Università di Milano Bicocca, Piazza della Scienza 3, 20126 Milano, Italy. E-mail: tara.desai@mib.infn.it

the order of milliseconds) to damage the specimens. Therefore this technique produces images of the live specimens (Foster *et al.*, 1992; Stead *et al.*, 1992) and it is also not influenced by the movement of the specimen. The images are obtained by exposing the specimens as a 1:1 radiograph on a photo resist which is then chemically developed and finally analyzed using an atomic force microscope (AFM). In this way no optics are required. This is significant because in the soft X-ray region, optics are still expensive and not very efficient. X rays in the water window range can be produced using low and high *Z* materials as targets. There are certain advantages of using a high *Z* target for producing X rays as X-ray conversion efficiency is high and copious soft X rays are generated due to Bremsstrahlung and recombination processes. However, there is a large spillover of radiation around the water window in the case of high *Z* materials.

In this article, we report the analysis of SXCM images of living *C. elegans*. The X-ray spectra that irradiated the specimens were also recorded using X-ray spectrometers. These spectra were used to obtain the corresponding plasma parameters like plasma density and temperature by spectroscopic analysis. Images obtained on the polymethilmetacrylate (PMMA) photo resists are analyzed using an AFM operating in contact mode. SXCM has already been used to image biological specimens like yeast cells, unicellular green algae, human red cells (Stead *et al.*, 1995*b*; Masini *et al.*, 1997; Batani *et al.*, 1998; Bortolotto, 2000). The experiments reported in the present article allowed us to explore the potentialities of this technique to study complex, multicellular organisms. To this aim, the biologically well characterized nematode *C. elegans* has been chosen. It is the first time that small (semimicroscopic) but complex (but not too complex, like mammals), multicellular samples have been studied by means of SXCM.

2. EXPERIMENTAL

X-ray microscopy experiments were performed using the Prague Asterix Iodine Laser System (PALS; Jungwirth *et al.*, 2001), which emits 1.314-μm radiation. Laser pulse duration was ~400 ps. The maximum optical energy in a single beam was ~600 J and the beam diameter at the entrance of the plasma chamber was ~290 mm. Laser radiation was focused on the target surface using a $f = 600$ mm focusing lens and the intensity was varied in the range $\sim 10^{14}$–10^{16} W/cm^2 by either changing the laser spot area (focal spot was varied from 150 μm to 600 μm) or changing the incident laser energy. The interaction chamber was evacuated to better than 10^{-4} mbar.

2.1. X-ray spectroscopy

Biological specimens were irradiated with X rays produced from three types of planar solid targets, Teflon (CF_2), molybdenum (Mo), and gold (Au). Gold and molybdenum have similar flux in water window regime (Batani *et al.*, 2000). A flat crystal Bragg's spectrometer was used to record the spectrum emitted by the plasma. X-ray spectra can provide information on the properties of the plasma, in particular, plasma density and temperature during the process of X-ray emission, by the analysis of the spectral shape, spectral width, and position of different lines and their relative intensities (Tallents, 1987). Teflon targets have a particularly simple *K*-shell centered at 0.9 KeV and are particularly useful for such a diagnostic purpose.

The spectrometer used in the present experiment had a RbAp crystal ($2d = 2.6121$ nm). Time- and space-integrated X-ray spectra were recorded on Kodak DEF films. In the present experiment, the spectrometer was placed at a distance of 6.5 cm from the X-ray source at an angle of 75° to the laser axis. Spectrometer placing was restricted due to the presence of biological sample holders. Spectra were recorded for every exposure of the biological sample. A 100-μm slit was placed on the spectrometer. An aluminum foil of 5 μm acted as a filter for the Teflon target whereas a 14-μm aluminum foil was used for gold and molybdenum targets.

X rays are produced from the dense and coronal plasma of a laser-irradiated target. The process lasts over a time span (τ_x) comparable to laser pulse duration (τ). Actually, X-ray emission duration depends on the plasma dynamics. Rapid plasma expansion leads to faster cooling, thereby terminating the process of X-ray emission. For picosecond pulses as in our case, the duration of the soft X-ray component is comparable to the laser pulse length. X-ray emission consists of continuous and characteristic line emission determined by the target material. Continuum is produced due to free–free Bremsstrahlung and free–bound transitions in a partially ionized plasma from dense ($n_e > n_c$) and coronal plasma ($n_e \leq n_c$), and the line emission from highly excited target ions. This emission is mostly in the soft X-ray region (below a few kiloelectron volts) and has been largely investigated as a tool for plasma diagnostics. In the case of a molybdenum target, soft X-rays are from the *N* shell whereas for gold targets they are from *N* and *O* shells.

2.2. Biological specimens

Encouraged by our earlier results on SXCM experiments on unicellular organisms like yeast (Batani *et al.*, 2000), our interest in the present investigation was to establish the suitability of the SXCM technique to study multicellular living organisms. From this point of view, the *C. elegans* nematodes seem to be a suitable choice for the following reasons:

- they are quite well studied and represented in the literature;
- they can be easily grown at 20°C on agar plates or in liquid culture in the laboratory;
- they can be conserved in liquid culture;

https://doi.org/10.1017/S0263034603214051 Published online by Cambridge University Press

- their life cycle is approximately 3 days;
- they are quite resistant to environmental changes;
- it is easy to study them at various developing phases;

C. elegans is a small, up to approximately 1 mm in length and about 30 μm in diameter, free-living nematode with a remarkable anatomic simplicity. An adult nematode contains 959 somatic cells. Its natural environment is the soil where this organism feeds mainly on bacteria.

In the sample holders, a droplet of water containing some biological specimens was sandwiched between a silicon nitride window and a photo resist (PMMA) with the minimum level of fluid (water), a little more than the specimen body diameter. The assembly of the specimen holder was similar to that of earlier works (Batani *et al.*, 2000). X rays were incident on the silicon nitride window, which is transparent to visible and X radiation. Usually 4–5 specimens were simultaneously exposed to every laser shot. The sample holders were placed at two different distances (5–10 cm from the X-ray source) at an angle of 45° to the laser axis. X rays are absorbed from various parts of specimen in different levels. Therefore different parts of the photo resist receive different X-ray doses, and the damage of the structure of the PMMA is affected by the characteristics of the sample. The chemical development of the photo resist gives rise to a profile of the sample, the height of which is proportional to the absorbed X-ray intensity. The height of the nematode profile is approximately 400 nm and the traces of the internal organs are of the order of 10–12 nanometers superimposed on this layer. Such a profile has been analyzed using AFM.

2.3. AFM analysis

Photo resists were analyzed using an Auto Probe CP Research AFM (ThermoMicroscopes, Sunnyvale, CA). All the AFM measurements discussed in the following were made in air operating in constant force mode. Microfabricated V-shaped silicon cantilevers with a silicon conical tip of resonant frequency of approximately 45 kHz and a force constant of 0.4 N/m were used. AFM images were processed using the Image Processing Data Analysis 2.0 software provided by ThermoMicroscopes.

In constant force mode, while the scanner gently traces the tip across the sample surface, the forces between tip and sample cause the cantilever to bend to accommodate changes from the sample topography. The spatial variation of the cantilever deflection can be used as input to a feedback circuit that moves the scanner up and down in the *Z* direction responding to the topography by keeping the cantilever deflection constant, and the topography images are generated using the signal applied to the scanner. In this operating mode, the speed of scanning is limited by the response time of the feedback circuit, but the total force exerted on the sample by the tip is well controlled so that this mode is generally preferred for most applications.

3. RESULTS AND DISCUSSION

3.1. Analysis of X-ray emission spectra

The X-ray spectra discussed in the following have been recorded at a laser intensity $I \sim 10^{14}$ W/cm^2 on target. X-ray intensities as a function of X-ray wavelength from Teflon, gold, and molybdenum plasmas are shown in Figure 1a, b, and c, respectively. X-ray intensities were corrected by taking into account the X-ray film response (Rockett *et al.*, 1985), crystal reflectivity (Henke *et al.*, 1985), and protective foil transmission (Henke *et al.*, 1986). Prominent and separated satellite lines were observed at lower photon energy for Teflon plasma as seen in Figure 1a ($\lambda > 15$ Å).

Spectra were analyzed by assuming purely free–free and free–bound transitions, which is a rather crude assumption in the present case. Results show that the X-ray intensity corresponds to an exponential decrease with increasing photon energy. The electron temperature for gold from the slope of the continuum (Fig. 1b) $T_e = 90 \pm 10$ eV. The analogous evaluation of the continuum emitted by the molybdenum plasma (Fig. 1c) shows a temperature $T_e = 120 \pm 10$ eV. The dominant bound–bound transitions are marked for Teflon plasma in Figure 2. Spectra clearly show H-like and He-like groups of lines and strong satellite lines. From these lines we can estimate the plasma density and temperature that characterize the plasma during the process of X-ray emission.

Laser-produced plasma is inhomogeneous. X rays are generated from different parts of the plasma that corresponds to different densities and temperatures as it expands from the target surface. Therefore a single temperature and density should not be appropriate to characterize such plasmas. However, we tried to interpolate experimental spectra using the minimum number of parameters, that is, a single density and a single temperature that must then be considered as a space

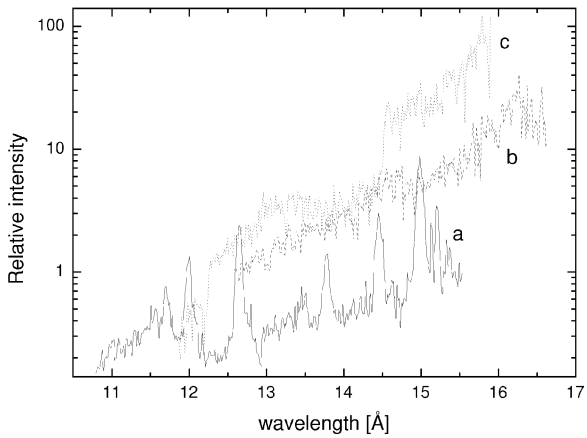

Fig. 1. X-ray intensity versus X-ray wavelength for (a) Teflon, (b) gold, and (c) molybdenum. Laser intensity on the target surface was 5×10^{14}, 2.6×10^{14}, 2.75×10^{14} W/cm^2, respectively. Al filter thickness was 5 μm for Teflon and 14 μm for Au and Mo.

https://doi.org/10.1017/S0263034603214051 Published online by Cambridge University Press

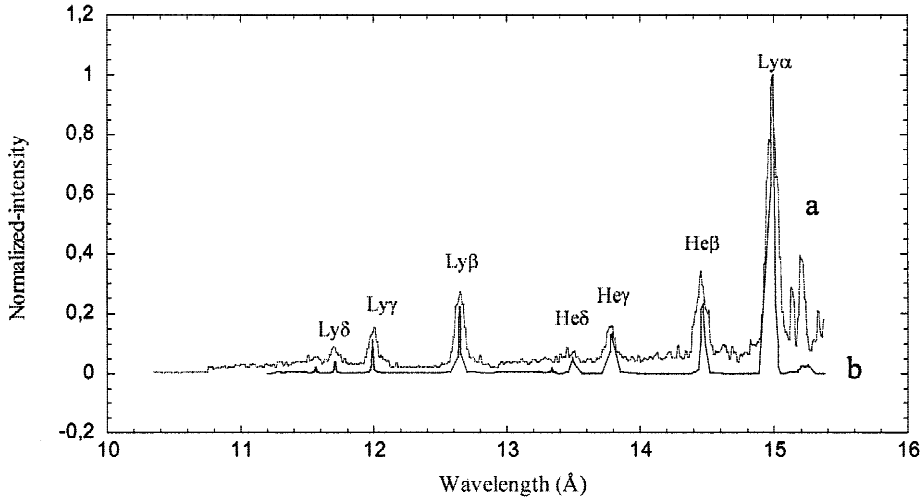

Fig. 2. Normalized X-ray intensity versus X-ray wavelength for Teflon target: (a) experimental results, (b) calculated by RATION.

and time average of the evolving plasma parameters during the process of X-ray emission. Line radiation and continuum are emitted due to different mechanism in the plasma. Line radiation is emitted due to the electron transition between bound states of an ion. The spectrum of the emitted radiation therefore consists of lines at distinct wavelengths, whereas the free–free transition and free–bound electron transitions give rise to continuum. In the present case, carbon *K*-shell emission was not recorded, as the lines were below the detectable range of the RbAP crystal. However, the presence of carbon (33%) in Teflon plasma implies the existence of carbon lines and recombination radiation due to carbon plasma. This can be seen as a continuum superimposed on fluorine ion lines. The continuum appearing at higher energy is mainly due to fluorine ions. The exponential interpolation of the continuum at high photon energy from Teflon spectra shows an average plasma temperature $T_e = 125 \pm 5$ eV.

In multiply charged ions, satellite lines appear when two electrons are in excited quantum states. One of the electrons undergoes a transition resulting in the emission of a photon, while the other, known as a spectator electron, remains in an excited quantum state, thereby affecting the energy levels of the excited quantum state. These satellite lines appear at a wavelength longer than the resonance lines. A shift in the wavelength depends on the excited state of the spectator electrons, and several satellites can be emitted depending on the excited state of the spectator electrons.

We also used the code RATION to synthesize X-ray spectra. This code was developed by R. Lee at the Lawrence Livermore National Laboratory (Lee, 1990) and used to generate *K*-shell spectra from carbon ($Z = 6$) to iron ($Z = 26$). Experimentally recorded Teflon spectra correspond to the X-ray wavelength in the range 10–16 Å. The calculations assumed fluorine ions ($Z = 9$) with 33% impurity from carbon, spot size of the order of laser focal spot on the target surface (150 μm), and instrumental width (FWHM) of 2 eV. Plasma was considered to be in nonlocal thermodynamic equilibrium (NLTE). Figure 2 shows (a) experimental and (b) synthetic spectra. The synthetic spectra show a quite good agreement with the experimental spectrum. Ly-β, He series, and Ly-α can be reproduced at $T_e = 145$ eV and plasma density $N_e = 4.8 \times 10^{20}/\text{cm}^{-3}$. However, the structure of the satellite lines is not well reproduced.

3.2. Biological images

Two AFM topography images of SXCM imprints on PMMA photo resists of *C. elegans* nematodes are shown in Figure 3. In particular, Figure 3a shows regularly repeating bands (ranging from 0.9 to 1.2 μm) giving rise to a structural periodicity along all the nematode profile. Both the well-defined pattern and the good agreement between our measurements and data reported in literature (Cox *et al.*, 1981) suggest that annuli of the nematode cuticle have been imaged. During the 3 days development of the specimen, the cuticle is replaced at each of four postembryonic molts. Literature data report that the cuticles of these developmental stages of *C. elegans* differ substantially from one another in ultrastructure and protein composition (Cox *et al.*, 1981). As the organism grows, the cuticle formed at each successive stage becomes thicker. The increase in cuticle thickness is proportional to the increase in body diameter during these stages. In the Juvenile J1, J4, and adult, the ratio of cuticle thickness to body diameter averages approximately 1:88.

The anterior body end of a *C. elegans* is shown in Figure 3b. The small protrusions, visible in the AFM image, are very similar in shape to the lips that symmetrically surround the buccal cavity of *C. elegans*.

The features of the image shown in Figure 4 have been obtained in various samples. AFM images collected in the

https://doi.org/10.1017/S0263034603214051 Published online by Cambridge University Press

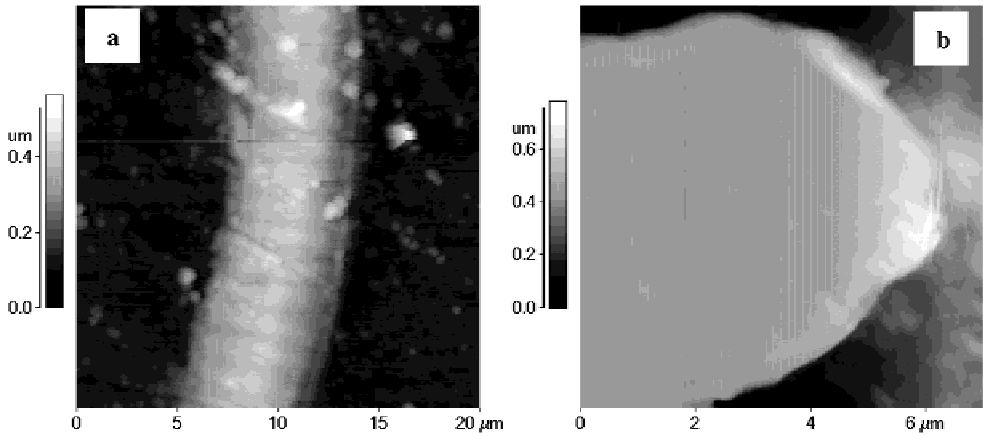

Fig. 3. AFM topography images of SXCM imprints on a PMMA photo resist of a *Caenorhabditis elegans*. (a) The nematode cuticle is circumferentially indented at regular approximately 1.1 μm intervals, creating pleated-appearing annuli. (b) Profile of the anterior body end.

central region of the nematode show a well-defined relief separating two regions with different roughnesses.

Several AFM images collected in the central region of the SXCM imprint of the *C. elegans* nematode showed structures morphologically well characterized presented in Figure 5. The comparison with data reported in literature (Bargmann & Avery, 1995) allowed us to regard them as nuclei of three different cell types. In particular, Figure 5a shows round hypodermal and gut nuclei with a large and prominent nucleolus, and Figure 5b shows neuronal nuclei that are round, small, and lacking in prominent nucleoli. The structures in Figure 5c can again be considered as cell nuclei (muscle nuclei?).

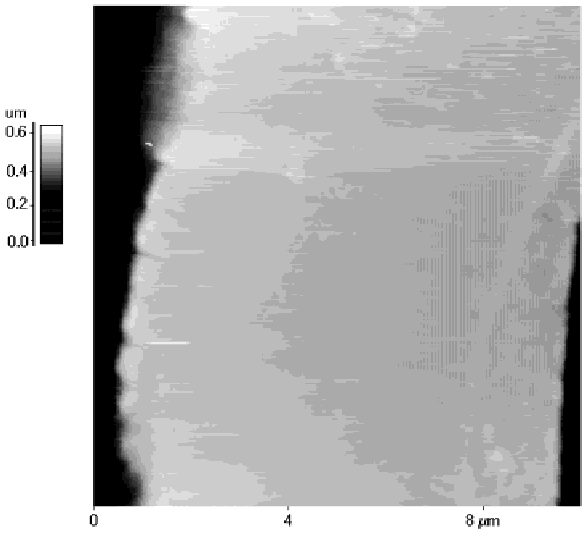

Fig. 4. A 10×10 μm^2 AFM topography image of a SXCM imprint on a PMMA photo resist of a *Caenorhabditis elegans*. This image has been collected at the central region of the body.

The present experimental data indicate our preliminary results. *C. elegans* of different sizes and in different development phases (length ranging from 250 to 1000 μm and corresponding diameters ranging from 10 to 30 μm) were present. As a consequence, the thickness of water around the various specimens was not constant. This may have influenced the quality of several images. Nevertheless good results are obtained from *C. elegans* of different dimensions, confirming that the technique can be used as a research tool top imaging non unicellular organism.

In spite of the large number of specimens (60 approximately) exposed to the X rays, about 20% have been recorded on the PMMA photo resist. Apart from the breakage of several extremely delicate silicon nitride windows during the various phases of the experiment, the probability of imaging a single *C. elegans* on the PMMA windows was low. Moreover, only a few photo resists showed identifiable structures. In spite of the above difficulties, the recorded images provide important quantitative information

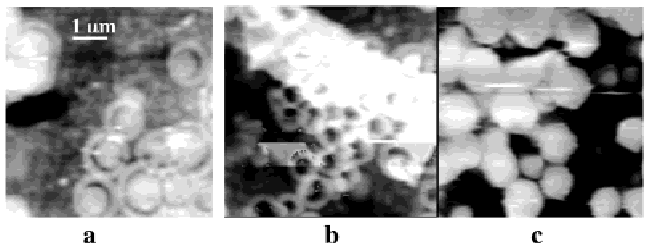

Fig. 5. Some 6×6 μm^2 AFM topography images of a SXCM imprint on a PMMA photo resist of a nematode *Caenorhabditis elegans*. The images have been collected in the central region of the nematode. Nuclei of three different cell types have been individuated: (a) hypodermal and gut nuclei, round with a large, prominent nucleolus; (b) neuronal nuclei, smaller, round, and without prominent nucleoli; (c) nuclei of a not individuated cell type.

https://doi.org/10.1017/S0263034603214051 Published online by Cambridge University Press

on *C. elegans*. Other images of the *C. elegans* will be published in detail elsewhere.

4. CONCLUSIONS

It is the first time that SXCM has been applied to the study of a multicellular living organism such as *C. elegans*. Internal structures and cuticle features of *C. elegans* have been distinguished. In spite of several problems encountered during the experiments, our preliminary results prove that the technique can be a useful tool in biological research. The knowledge and control of experimental parameters such as the water layer thickness, the X radiation intensity, the device geometry, the photo resist chemical development, and the sex and embryonic development of the biological specimens will allow us to obtain better results in the future.

From the experimental spectra, we observe many X rays at higher energy ($h\nu \geq 1$ KeV) that can penetrate the sample. The fact that we used infrared laser radiation and high Z target materials could indeed justify a strong X emission outside the water window. This can explain the low contrast found in many AFM images.

REFERENCES

Bargmann, C.I. & Avery, L. (1995). Laser Killing of cells in Caenorhabditis elegans. *Methods Cell Biol.* **48**, 225–249.

Batani, D., Masini, A., Lora Lamia Donin, C., Cotelli, F., Previdi, F., Milani, M., Faral, B., Conte, E., Moret M., Poletti, G. & Pozzi, A. (1998). Characterisation of Saccharomyces cerevisiae yeast cells. *Phys. Medica* **15**, 151–157.

Batani, D., Botto, C., Bortoloto, F., Masini, A., Bernardinello, A., Moret, M., Milani, M., Eidmann, K., Poletti, G., Cotelli, F., Donin, C.L.L., Piccoli, S., Stead, A., Ford, T., Marranca, A., Flora, F., Palladino, L. & Reale, L. (2000). Contact X-ray microscopy using the Astrix laser source. *Phys. Medica* **16**, 49–55.

Bortolotto, F., Batani, D., Masini, A., Previdi, F., Rebonato, L. & Tureu, E. (2000). Study of a X-ray laser-plasma source for radiobiological experiments, microdosimetry analysis and plasma characterisation. *Euro. Phys. J. D* **11**, 309.

Cox, G.N., Staprans, S. & Edgar, R.S. (1981). The cuticle of Caenorhabditis elegans. *Dev. Biol*. **86**, 456–470.

Fletcher, J., Cotton, R.A. & Webb, C. (1992). Soft x-ray contact microscopy using laser generated plasma sources. *Proc. SPIE* **1741**, 142–153.

Ford, T.W., Stead, A.D. & Cotton R.A. (1991). Soft x-ray contact microscopy of biological materials. *Electron Microsc. Rev*. **4**, 269–292.

Ford, T.W., Page, A.M., Foster, G.F. & Stead, A.D. (1992). Effects of soft x-ray irradiation on cell ultrastructure. *Proc. SPIE* **1741**, 325–332.

Foster, G.F., Buckley, C.J., Bennett, P.M. & Burge, R.E. (1992). Investigation of radiation damage to biological specimens at water window wavelengths. *Rev. Scient. Instr*. **63**, 599–600.

Henke, B.L. & Jaanimagi, P.A. (1985). Two-channel, elliptical analyzer spectrograph for absolute, time-resolving time-integrating spectrometry of pulsed x-ray sources in the 100–10000-eV region. *Rev. Sci. Instrum*. **56**, 1537–1552.

Henke, B.L. (1986). Low-energy x-ray response of photographic films. Mathematical models. *J. Opt. Soc. Am. B* **3**, 11, 1540–1546.

Jungwirth, K., Cejnarova, A., Juha, L., Kralikova, B., Krasa, J., Drousky, E., Krupickova, P., Laska, L., Masek, K., Mocek, T., Pfeifer, M., Präg, A., Renner, O., Rohlena, K., Rus, B., Skala, J., Straka, P. & Ullschmied, J. (2001). The Prague Astrix Laser System. *Phys. Plasmas* **8**, 2495–2501.

Kondo, K. & Tomie, T. (1994). Optimization of a laser-plasma X-ray source for contact X-ray microscopy. *J. Appl. Phys*. **75**, 3798–3805.

Lee, R.W. (1990). *User Manual for RATION*. Livermore, CA: Lawrence Livermore National Laboratory.

Masini, A., Batani, D., Previdi, F., Conti, A., Pisani, F., Botto, C., Bortolotto, F., Torsiello, F., Tureu, E., Allot, R., Lisi, N., Milani, M., Costato, M., Pozzi, A. & Koenig, M. (1997). X-ray irradiation of yeast cells. *Proc. SPIE* **3157**, 203–217.

Nobel Foundation. (2002). The Nobel Prize in Physiology or Medicine. Press Release, October 7.

Stead, A.D., Cotton, R.A., Page, A.M., Dooley, M. & Ford, T.W. (1992). Visualization of the effects of electron microscopy fixatives on the structure of hydrated epidermal hairs of tomato (Lycopersicum peruvianum) as revealed by soft X-ray contact microscopy. *Proc. SPIE* **1741**, 351–362.

Stead, A.D., Page, A.M., Cotton, R.A., Neely, D., Bagby, R., Miura, E., Tomie, T., Shimizue, S., Majima, T., Anastasi, P.A.F. & Ford, T.W. (1995*b*). Modifications for soft X-ray contact microscopy-quantification of carbon density discrimination and stereo imaging. *Proc. SPIE* **2523**, 202–211.

Stead, A.D., Page, A.M. & Ford, T.W. (1995*a*). The prospects for soft X-ray contact microscopy using laser plasmas as a X-ray source. *Proc. SPIE* **2523**, 40–50.

Rockett, P.D., Bird, C.R., Hailey, C.J., Sullivan, D., Brown, D.B. & Burkhalter, P.G. (1985). X-ray calibration of Kodak Direct Exposure film. *Appl. Opt*. **24**, 2536–2542.

Tallents, G.J. (1987). X-ray spectroscopy of tokamaks. JET Report No. JET-P(87) 56.